Materials Letters 255 (2019) 126582

Contents lists available at ScienceDirect

Materials Letters

journal homepage: www.elsevier.com/locate/mlblue

Piezoresistive geopolymer enabled by crack-surface coating

Shikun Chen [a], Yanxiao Li [b,1], Dongming Yan [a], Chenglin Wu [b,*], Nicholas Leventis [c]

[a] College of Civil Engineering and Architecture, Zhejiang University, Hangzhou 310058, PR China
[b] Department of Civil, Architectural, and Environmental Engineering, Missouri University of Science and Technology, Rolla, MO 65409-0030, USA
[c] Department of Chemistry, Missouri University of Science and Technology, Rolla, MO 65409-0030, USA

ARTICLE INFO

Article history:
Received 12 June 2019
Received in revised form 1 August 2019
Accepted 22 August 2019
Available online 23 August 2019

Keywords:
Geopolymer
Conductive polymer
Contact mechanics
Piezo-resistance
Self-sensing

ABSTRACT

The conductive polymer was introduced to crack surfaces in geopolymers to enable piezo-resistivity. In combination with crack morphology characterization and the piezo-resistive test, the functionalized geopolymer was found to achieve a high sensitivity (with $\Delta R/R_0/\Delta\varepsilon$ equals to 376.9 for loading and 513.3 for unloading) to both small external stress (less than 2 MPa) and wide range of strains (up to 1700 με). This piezo-resistive behavior can be well described by a coupled mechanical-conductive contact mechanism. A new way to enable the self-sensing function of materials utilizing their existing micro-features was successfully proposed and validated.

1. Introduction

Self-detection of internal strains is critical in next-generation structural health monitoring system for buildings constructed using eco-friendly materials such as geopolymers. To realize such functionality, the intrinsic piezo-electricity [1,2] and filler-enabled piezo-resistivity [3–7] are usually applied. However, these approaches face limitations in intrinsic sensitivity and difficulties in filler-dispersions [8,9]. To overcome these obstacles, present work utilizes the coupled-mechanical-conductive contact mechanism to enhance the sensitivity of the piezo-resistive behaviour. By combining a conductive polymer coating and natural crack features, the proposed approach shows a high sensitivity in modified geopolymers. Further theoretical analysis based-on the underlying physics also provide a well-established calibration procedure and shed-light on next-generation self-sensing construction materials.

2. Experimental

2.1. Materials

The geopolymer was synthesized with 0.56 g/ml commercial metakaolin (OPTIPOZZ, MK-750, 51.93% SiO_2, 44.94% Al_2O_3), 1.05 g/ml liquid sodium silicate (PQ, N Type, 8.9% Na_2O, 28.7% SiO_2) and 0.08 g/ml sodium hydrate (Sigma-Aldrich, reagent grade, >98%). The paste has a chemical composition of Na/Al = 1.0, Si/Al = 2.0 and H_2O% = 39.83 wt%. The commercial conductive polymer PEDOT: PSS (Sigma-Aldrich, conductive grade, 1.3 wt% in H_2O) was adopted as the coating material (Scheme 1).

2.2. Sample preparation

The binder was mixed and casted into 10 mm cubic molds. It was sealed and hardened under 60 °C for 24 h and cured under 20 °C for 7 d. The artificial crack was introduced by cutting and cleaving the sample in the middle. Two copper electrodes were glued around the side surfaces with silver epoxy. The PEDOT: PSS solution was then coated onto the crack and side surfaces with a solute dosage about 10 μg/mm^2. The coating was dried under 45 °C for 30 min. To prepare naturally-cracked samples, the cubes were dried under 150 °C for 20 min to form networked cracks. It was then immersed into PEDOT: PSS solution (0.5 wt%) and dried subsequently under 45 °C for 30 min.

2.3. Compressive piezo-resistivity experiment

The compressive piezo-resistivity was measured by voltammetry method (Fig. 1(a)). The current (under 10 V DC voltage) and uniaxial compression force (up to 200 N at rate of 0.1 mm/min) were monitored by National Instruments 9208 module and MTS Universal Tester. The average crack closure and strain were measured by digital image correlation (DIC) at a gauge length of 8 mm.

* Corresponding author.
E-mail address: wuch@mst.edu (C. Wu).
[1] This contributed equally to the first author.

https://doi.org/10.1016/j.matlet.2019.126582
0167-577X/

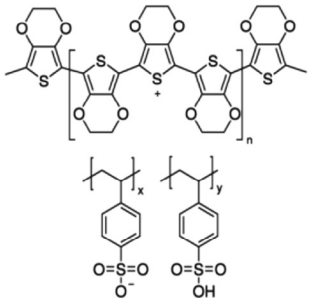

Scheme 1. Structure of PEDOT: PSS.

2.4. Crack surface characterization

The morphology of coated crack surface was characterized using optical microscope-based three-dimensional profilometer (Hirox, KH-8700). The micro-features of the crack surface were observed using scanning electron microscope (Helios Nano Lab 600 FIB/SEM, Thermo Fisher Scientific) and atomic force microscope (AFM, Digital Instruments, Multimode 3).

3. Results and discussions

3.1. Piezo-resistivity of artificially-cracked sample

The mechanical contacts at randomly distributed asperities function as many variable electrical resistors (Fig. 1(b)). As shown in Fig. 1(c, d), the electrical resistance of full sample decreases as external load increases (Fig. 1(c)). The relative resistance $\left(\frac{R}{R_0}\right)$ was plotted against the crack closure (Δd) from Eq. (1):

$$\Delta d = d - d_0 = \Delta L - L\frac{p}{E} \tag{1}$$

where d_0 is the initial crack spacing; d is the current crack spacing from DIC measurement; Δd is the crack closure; ΔL is the gauge deformation; $L = 8$ mm is the gauge length; $p = P/A$ is the nominal pressure, P is the external load, $A = 8 \times 8$ mm^2 is the nominal contact area; $E = 3.87$ GPa is the elastic modulus of geopolymer without cracks.

The $\frac{R}{R_0}$ decreases to 51%–67% as the crack closure reaches to 40 μm, approximately, which yields an average sensitivity $\left(\frac{\Delta R}{R_0}/\Delta d\right)$ of 0.98%/μm.

3.2. Crack surface morphology

The surface morphology of the artificial crack was shown in Fig. 2. The surface has a global curvature along with many local roughness (Fig. 2(a)). The optically measured two opposite surfaces were shown in Fig. 2(b). Fig. 2(c) shows the cross-sectional profiles along the dash-lines shown in Fig. 2(b). The mean radius of curvature at asperity peaks was about 240 μm. The combined height of these surfaces is calculated as Eq. (2), which has a mean value of zero and standard deviation (σ_h) of 99.93 μm.

$$h = h_1 + h_2 \tag{2}$$

where h_1 and h_2 are asperity heights around the global curvature extracted from the optical surface morphologies.

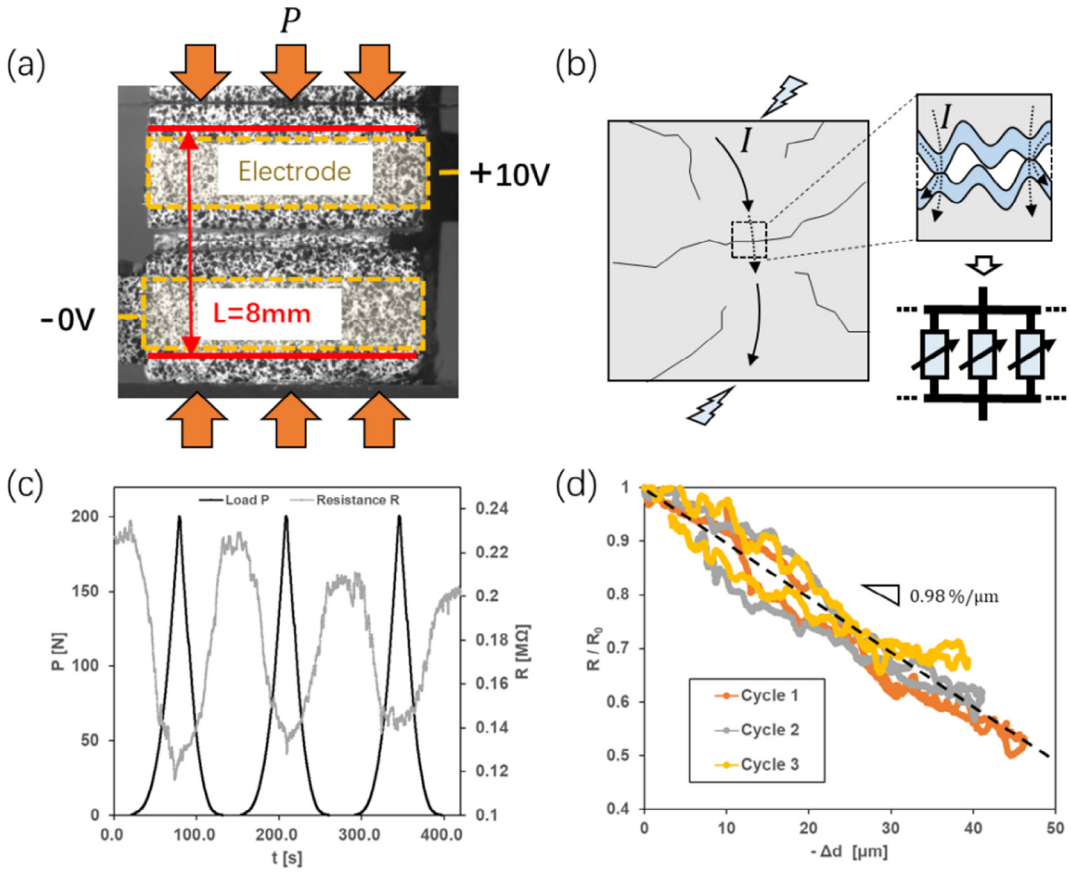

Fig. 1. (a) Piezo-resistance experiment of artificially-cracked sample; (b) crack-based sensing mechanism that utilize the contact asperities as adjustable resistance; (d) temporal variation of applied load and resistance response (d) relative resistance variation versus the crack closure.

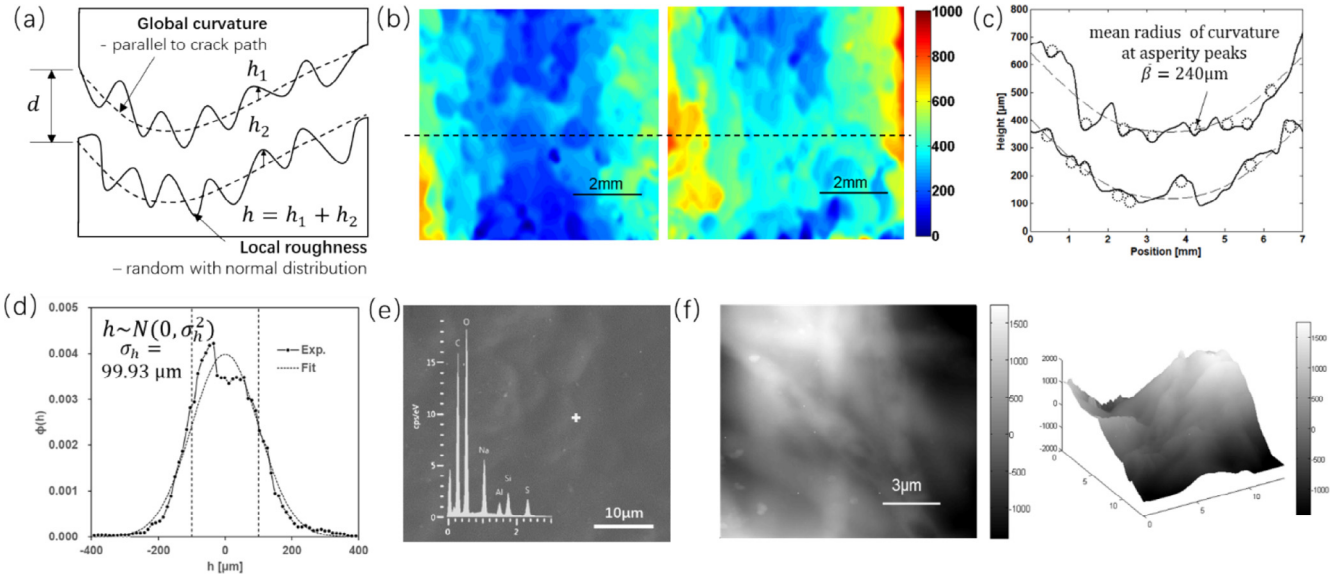

Fig. 2. (a) Illustration of crack surface morphology; (b, c) macro crack surface profile from optical profilometer; (d) distribution of the combined asperity height; (e) SEM morphology showing the smooth PEDOT: PSS coating on crack surface; (f) AFM morphology showing small roughness with a height within ±2000 nm.

The finer surface features could be seen from the SEM in Fig. 2 (e) and AFM (Fig. 2(f)) observation. The results show a smooth surface profile for the PEDOT: PSS coated crack.

3.3. Analytical model of single-crack piezo-resistivity

To understand the piezo-resistivity of the sample with artificial single-crack, a Hertzian contact model was first used (Fig. 3). The contact of each asperity-pair was modelled as two contacting elastic hemispheres with radii equal to the mean radius of curvature at asperity peaks. The relationship between contact area ratio and applied force is then [10,11],

$$\frac{A_c}{A} = \pi^2(\eta\beta\sigma_h)^2 F_2\left(\frac{d_0 + \Delta d}{\sigma_h}\right) \tag{3}$$

where A is the nominal contact area; A_c is the real contact area; η is the asperity density (number/area); β is the mean radius of curvature at asperity peaks; σ_h is the standard deviation of the combined asperity height.

The function $F_2(u)$ shown in Eq. (3) is an integral function which relates to the distribution of the combined asperity height [10],

$$F_2(u) = \int_u^{\infty} (s-u)^n \phi^*(s) ds \tag{4}$$

where, $s = \frac{h}{\sigma_h}$, which follow the standard normal distribution $N(0,1)$; $\phi^*(s)$ is the standardized normal distribution.

The electrical resistance due to the constriction of the contact area could be estimated from the Holm model [12,13],

$$R_c = \frac{\rho}{2r} \tag{5}$$

where, $r = \sqrt{\frac{A_c}{\eta A \pi}}$ is the equivalent Holm contact radius of the constricted area; and ρ is the conductivity of the basic material.

We then estimate the relative resistance due to contact area constrictions as

$$\frac{R_c}{R_{c,0}} = \frac{r_0}{r} = \sqrt{\frac{A_{c,0}}{A_c}} \tag{6}$$

Assuming the total resistance (R) was composed of the variable constriction resistance (R_c) and the invariant matrix resistance (R_m), that is $R = R_m + R_c$,the total relative resistance is,

$$\frac{R}{R_0} = \frac{R_m + R_c}{R_m + R_{c,0}} = \frac{\zeta + \frac{R_c}{R_{c,0}}}{\zeta + 1} \tag{7}$$

where $\zeta = \frac{R_m}{R_{c,0}}$.

Fig. 3(c) shows the close agreement between the model and experiments with $d_0 = 3\sigma_h$, $\zeta = 0.3$, 0.4 and 0.6.

3.4. Piezo-resistivity of naturally-cracked sample

To further demonstrate the proposed sensing mechanism, a sample with naturally formed cracks and PEDOT: PSS coatings (Fig. 3(b)) was tested.

As previous artificially-cracked sample, the resistance has an obvious decrease with compression. The first and last 25% of the curve could be fitted with a linear relationship and the average sensitivity $\left(\frac{\Delta R}{R_0}/\Delta\varepsilon\right)$ of these parts are 376.9 and 513.3 respectively (Fig. 3(d)).

The previous single-crack model could be further extended to multi-cracks condition. The strain of the sample has a relation with the crack displacement as

$$\varepsilon = \xi\varepsilon_c + (1-\xi)\varepsilon_m = \xi\frac{\Delta d}{d_0} + (1-\xi)\frac{p}{E} \tag{8}$$

where, ε is the total strain, ε_c is the local strain at the cracks, ε_m is the elastic strain of uncracked parts, ξ is the homogenous factor related to the crack density.

Through Eq. (8) with $d_0 = 3\sigma_h$, we could estimate the crack deformation from the measurements as

$$\frac{\Delta d}{\sigma_h} = \frac{3}{\xi}\left[\varepsilon - (1-\xi)\frac{p}{E}\right] \tag{9}$$

Then, using previously described single-crack model and parameters ($\xi \approx 0.006$, $\zeta \approx 0$), the relative resistance could be estimated.

As shown in Fig. 3(d), experimental and analysis results show a good agreement during the initial loading stage before the applied strain reaches 1700 με. Similar agreement was also observed during the unloading stage for the strains ranging from 2300 με to 4000 με. However, the relatively poor agreements were observed for large strains under which the plastic deformation dominates the contacts. Still, this work demonstrated the feasibility of the

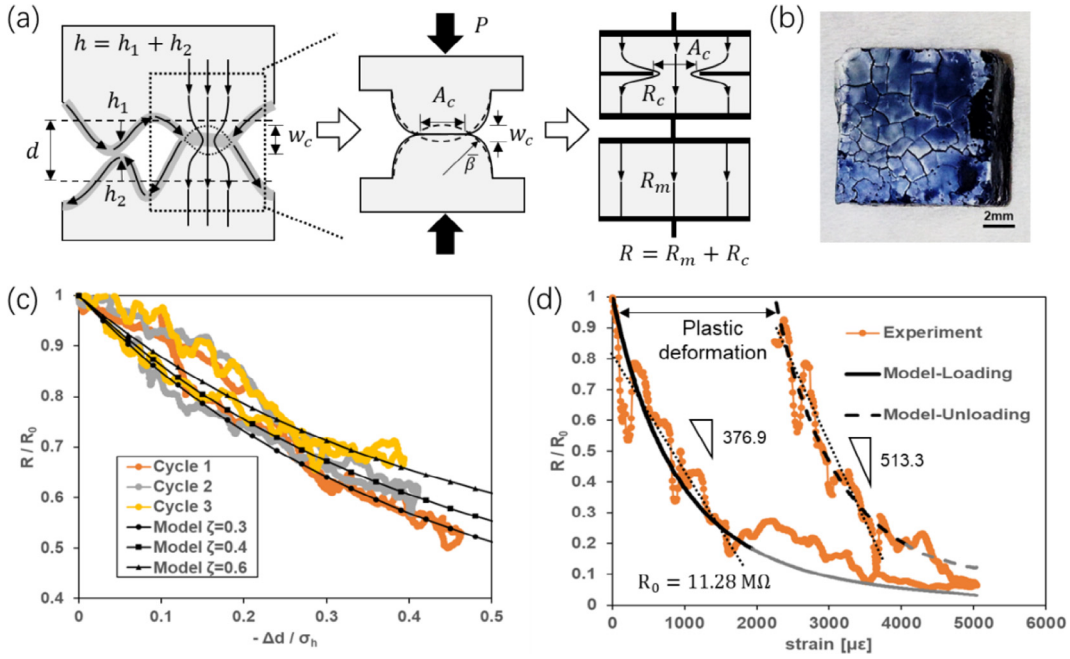

Fig. 3. (a) Illustration of mechanical and electrical contact mechanism; (b) natural cracked sample with PEDOT coating; (c, d) comparison of piezo-resistive behavior of artificial cracked and natural cracked sample to model estimations.

proposed sensing mechanism. Further improvement could also be made by optimization of features related to parameters shown in proposed models.

4. Conclusion

This work explored and demonstrated the feasibility of utilizing the coupled-mechanical-conductive contact mechanism to achieve self-sensing functionalization of geopolymers. Using conductive PEDOT: PSS coating on crack surface, the modified geopolymer has shown a high sensitivity (with $\frac{\Delta R}{R_0}/\Delta\varepsilon$ equals to 376.9 and 513.3 for loading and unloading process, respectively) to both small external stress (less than 2 MPa) and wide range of strains (up to 1700 με). The analytical model has been developed and shown that the piezo-resistivity of both artificially and naturally cracked sample could be estimated according to the crack morphology information. This also shows the robustness of the proposed functionalization mechanism. However, it should be pointed out that the potential environmental effects such as moisture and chemical ingress can significantly affect the proposed sensing mechanism, which will be investigated in the future work.

Declaration of Competing Interest

The authors declare that they have no known competing financial interests or personal relationships that could have appeared to influence the work reported in this paper.

Acknowledgements

The author would like to thank graduate research assistant, Chuanrui Guo, at Missouri University of Science and Technology for his assistance during the uniaxial compression experiments. This work is financially supported by Center for Infrastructure Engineering Studies at Missouri S&T, and Missouri Department of Transportation under contract of TR202008.

Appendix A. Supplementary data

Supplementary data to this article can be found online at https://doi.org/10.1016/j.matlet.2019.126582.

References

[1] C. Lamuta, S. Candamano, F. Crea, L. Pagnotta, Mater. Des. 107 (2016) 57–64.
[2] M. Saafi, A. Gullane, B. Huang, H. Sadeghi, J. Ye, F. Sadeghi, Compos. Struct. 201 (2018) 766–778.
[3] M. Saafi, K. Andrew, P.L. Tang, D. McGhon, S. Taylor, M. Rahman, S. Yang, X. Zhou, Constr. Build. Mater. 49 (2013) 46–55.
[4] C. Lamuta, L. Bruno, S. Candamano, L. Pagnotta, MRS Adv. 2 (2017) 3773–3779.
[5] S. Bi, M. Liu, J. Shen, X.M. Hu, L. Zhang, ACS Appl. Mater. Interfaces 9 (2017) 12851–12858.
[6] P. Rovnaník, I. Kusák, P. Bayer, P. Schmid, L. Fiala, Materials (Basel) 12 (2019) 1616.
[7] L. Deng, Y. Ma, J. Hu, S. Yin, X. Ouyang, J. Fu, A. Liu, Z. Zhang, Constr. Build. Mater. 222 (2019) 738–749.
[8] J.L. Zhou, Y. Hu, V.W.Y. Tam, W. Li, Z. Tang, Constr. Build. Mater. 200 (2018) 474–489.
[9] W. Dong, W. Li, Z. Tao, K. Wang, Constr. Build. Mater. 203 (2019) 146–163.
[10] J.A. Greenwood, J.H. Tripp, Proc. Inst. Mech. Eng. 185 (1970) 625–633.
[11] H. Hertz, Lord Rayleigh, Misc. Pap. (J. Fur Die Reine Und Angew. Math.) 92 (1881) 146–162.
[12] L. Kogut, K. Komvopoulos, J. Appl. Phys. 94 (2003) 3153–3162.
[13] R. Holm, Electrical Contacts, fourth ed., Springer, New York, 1967.